arXiv:nucl-th/0404078v2 27 Apr 2004

Neutral-current neutrino-nucleus cross-sections for $A \sim 50 - 65$ nuclei

A. Juodagalvis [a,b,1], K. Langanke [c], G. Martínez-Pinedo [d,e], W.R. Hix [a,b], D.J. Dean [a], and J.M. Sampaio [c]

[a] *Physics Division, Oak Ridge National Laboratory, P.O. Box 2008, Oak Ridge, TN 37831-6373, USA*

[b] *The Department of Physics and Astronomy, University of Tennessee, Knoxville, TN 37996, USA*

[c] *Institut for Fysik og Astronomi, Århus Universitet, DK-8000 Århus C, Denmark*

[d] *Institut d'Estudis Espacials de Catalunya, Edifici Nexus, Gran Capità 2, E-08034 Barcelona, Spain*

[e] *Institució Catalana de Recerca i Estudis Avançats, Lluís Companys 23, E-08010 Barcelona, Spain*

Received 23 April 2004

Abstract

We study neutral current neutrino-nucleus reaction cross-sections for Mn, Fe, Co and Ni isotopes. An earlier study for a few selected nuclei has shown that in the supernova environment the cross sections are increased for low energy neutrinos due to finite-temperature effects. Our work supports this finding for a much larger set of nuclei. Furthermore we extend previous work to higher neutrino energies considering allowed and forbidden multipole contributions to the cross sections. The allowed contributions are derived from large-scale shell model calculations of the Gamow-Teller strength, while the other multipole contributions are calculated within the Random Phase Approximation. We present the cross sections as functions of initial and final neutrino energies and for a range of supernova-relevant temperatures. These cross sections will allow improved estimates of inelastic neutrino reactions on nuclei in supernova simulations.

Key words: Shell model; Random-Phase Approximation; Gamow-Teller transitions; neutral-current; weak-interactions; neutrino-nucleus reaction cross section; nuclear astrophysics.
PACS: 26.50.+x; 23.40.Bw; 21.60.Cs; 97.60.Bw

[1] e-mail: andrius@mail.phy.ornl.gov

1 Introduction

Neutrino-nucleus reactions play essential roles in many astrophysical applications. These include core-collapse supernovae [1], explosive [2] and r-process nucleosynthesis [3], and observation of solar and supernova neutrinos by terrestrial detectors [4].

Stars with masses $\gtrsim 10 M_\odot$ end their lives as core-collapse supernovae. In the final stages of their evolution these stars produce an inner core consisting of electrons and 'iron nuclei' (nuclei with mass numbers $A \sim 60$). As these nuclei have the highest binding energy per nucleon, additional fusion reactions cost, rather than generate, energy. The stellar core has lost its energy source, and once the core mass has grown larger than the Chandrasekhar mass limit the star starts to collapse under its own gravity. The simulation of the final evolution and collapse of such massive stars is one of the outstanding current challenges in astrophysics, combining state-of-the-art microphysics input (nuclear and neutrino physics) with sophisticated treatments of hydrodynamics and radiation transport. Despite significant progress in both of these aspects, current core-collapse supernova simulations often fail to yield explosions [5,6,7]. Since most of the explosion energy is carried by neutrinos, an essential part of these simulations is a detailed treatment of neutrino transport including the various interactions of neutrinos with the supernova environment. One of these interaction processes is inelastic neutrino-nucleus scattering, which is currently ignored in supernova simulations. Recent work indicates that this might be unjustified. It has been shown that finite temperature effects increase the low-energy neutrino-nucleus cross sections significantly [8]. Furthermore, recent improvements in calculating electron capture on heavy nuclei during the collapse phase implies that these captures dominate the capture on free protons [9,10], in contrast to previous beliefs [1,11]. Captures on nuclei produce neutrinos with smaller energies, making temperature effects more important, and the inclusion of inelastic neutrino-nucleus reactions in supernova simulations more relevant. A call for reliable neutrino-nucleus cross sections has also been made in the context of explosive nucleosynthesis, occurring when the shock wave passes through the exploding star which leads to fast nuclear reactions [2].

The pioneering study of neutrino-nucleus reactions during core collapse has been performed by Bruenn and Haxton [12]. These authors calculated inelastic neutrino-nucleus scattering rates (neutral current) and neutrino-nucleus absorption rates (charged current) approximating the nuclear composition present in the stellar core by a single nucleus, ^{56}Fe. The calculated rates were based on a nuclear model appropriate for temperatures $T = 0$, combining a truncated nuclear shell model evaluation of the allowed contributions to the cross sections with estimates for forbidden components within the framework of the Goldhaber-Teller model [12]. In detailed supernova simulations Bruenn and Haxton studied 3 phases of the collapse and explosion in which neutrino-nucleus reaction could be potentially important: the matter infall, the prompt shock propagation phase, and the delayed-shock phase. First, they found that inelastic neutrino-nucleus scattering plays the 'same extremely important role of equilibrating ν_e's to matter during infall as neutrino-electron scattering'

[12]. Second, they did not confirm an earlier suggestion by Haxton [13] who pointed to the possibility that neutrino-nucleus reactions can preheat the matter ahead of the shock during the early phase of the explosion. Third, their simulation indicated no significant contribution of neutrino-nucleus reactions to the revival of the stalled shock, compared to neutrino absorption on free nucleons.

Sampaio *et al* have argued that the finite temperature environment of a supernova alters inelastic neutrino-nucleus scattering cross sections noticeably [8]. Using a shell-model treatment of the dominant Gamow-Teller (GT) component they showed that finite-temperature effects increase the cross sections for inelastic neutrino scattering on even-even nuclei, like ^{56}Fe, at low energies ($E_\nu \lesssim 10$ MeV) significantly. On the other hand, their study of ^{56,59}Co and ^{59}Fe suggested that the effect is less pronounced for odd-A and odd-odd nuclei. This variation in the importance indicates that inelastic neutrino-nucleus cross sections for application in supernova simulations should be derived i) at finite temperatures and ii) for an appropriate matter composition. The aim of the present work is to prepare data on an ensemble of nuclei relevant for supernova simulations. Calculations have been performed for 40 isotopes of Mn, Fe, Co, and Ni, covering in each isotope chain the range from $N = Z$ to very neutron-rich nuclei. To estimate the possible effect of inelastic neutrino-nucleus scattering within a supernova, we use the calculated cross sections to speculate about the matter heating rate in the post-bounce supernova.

In a supernova, inelastic neutrino-nucleus scattering occurs at rather modest neutrino energies, $E_\nu \lesssim 50$ MeV. This makes the cross sections sensitive to nuclear structure effects, particularly for neutrinos with energies lower than 20 MeV. Therefore nuclear models must be employed, which can describe the many-body correlations in the nucleus accurately. The model of choice is the shell model, which now allows for virtually converged calculations of the Gamow-Teller response for nuclei in the iron mass range [14], with a quite satisfactory reproduction of the available experimental Gamow-Teller data [14,15,16,17]. While the GT component determines the neutrino-nucleus cross section at low neutrino energies, higher multipole contributions become increasingly important at higher neutrino energies. We have calculated these contributions within the Random Phase Approximation (RPA) [18].

This paper is organized as follows. In section 2 we briefly describe the formalism used to evaluate inelastic neutrino-nucleus cross sections at finite temperature. The results are presented in section 3. For each nucleus, the cross sections are shown for several representative supernova temperatures. Since the important quantity for supernova simulations is the energy transfer from neutrinos to the core matter, we present cross sections as a function of initial and final neutrino energies for representative nuclei. We finish the paper with a summary and conclusions in section 4. There we also make some remarks on the impact of our results on the matter heating rate in supernova simulations.

2 Models

In neutrino-induced reactions the nucleus is excited by multipole operators O_λ which scale like $(qR/\hbar c)^\lambda$, where R is the nuclear radius ($R \sim 1.2A^{1/3}$ fm). As the momentum transfer q is of the order of the neutrino energy E_ν, neutrino-nucleus reactions involve multipole operators with successively higher rank λ as the neutrino energy increases [4].

Inelastic scattering of low-energy neutrinos off nuclei is dominated by allowed ($\lambda = 0$) Gamow-Teller transitions. The GT response is in turn sensitive to nuclear structure effects and hence its contribution to the cross section has to be derived from a model which is capable to describe both the relevant nuclear structure and the correlation effects. This model is the diagonalization shell model [19]. The finite temperature in a supernova environment implies that the scattering occurs on a thermal nuclear ensemble rather than the ground state. However, the relevant supernova temperatures ($T \leq 2$ MeV) ensure that mainly states at modest nuclear excitation energies, which are also reasonably well described within large-scale shell model approaches, are present in the thermal ensemble. As we will show below, finite-temperature effects are only relevant for low neutrino energies ($E_\nu \lesssim 15$ MeV). Thus we expect that GT transitions will also dominate the neutrino scattering cross section on the thermally excited nuclear states at these neutrino energies.

Higher multipoles contribute to the cross section for larger neutrino energies. For each of these multipoles the response of the operator will be fragmented over many nuclear states. However, most of the strength resides in a collective excitation, the giant resonance, whose centroid energy grows with increasing rank λ roughly like $\lambda\hbar\omega \approx 41\lambda/A^{1/3}$ MeV. As the phase space prefers larger final neutrino energies, the average nuclear excitation energy grows noticeably slower than the initial neutrino energy. As a consequence, initial neutrino energies are noticeably larger than the energy of a giant resonance, when the latter will contribute to the neutrino-nucleus cross section. Fortunately, the neutrino-nucleus cross section depends then mainly on the total strength of the multipole excitation and its centroid energy, and not on the detailed energy distribution of the strength (as it is for the Gamow-Teller response at low neutrino energies). We will derive the higher multipole contributions to the neutrino-nucleus cross section within the RPA, making use of the fact that the RPA describes the energy centroid and the total strength of multipoles other than the Gamow-Teller quite well.

Kolbe *et al* [20] proposed this hybrid model, in which contributions of the allowed transitions ($\lambda = 0$) to the neutrino-nucleus cross section are derived within the shell model, and the other multipole responses ($\lambda > 0$) are calculated within the RPA. It has been shown that the model reproduces the experimental (ν_e, e^-) cross section on ^{56}Fe, induced by neutrinos with a Michel energy spectrum [20]. Toivanen *et al* applied this model to various neutrino-induced reactions on iron isotopes at the temperature $T = 0$ [21]. Unfortunately, no inelastic neutrino-nucleus scattering data for nuclei exists, except for the transition from the ground state to the isospin $T = 1$ state at $E_x = 15.11$ MeV in ^{12}C [22]. However, it was recently shown that

high-precision data on the magnetic dipole strength distribution, obtained from inelastic electron scattering on spherical nuclei, like ^{50}Ti, ^{52}Cr and ^{54}Fe, give the required information about the Gamow-Teller strength distribution for these nuclei and thus strongly constrain inelastic low-energy neutrino-nucleus cross sections [23]. The diagonalization shell model reproduces the electron scattering data very well, validating this model for calculation of low-energy inelastic neutrino-nucleus cross sections. Alternatively, the relevant GT_0 strength could be obtained through a complete isospin decomposition of the GT_- strength measured in (p,n)-type reactions, see [24]. Nevertheless a direct measurement of neutrino-nucleus cross sections for selected nuclei relevant for supernova simulations is desirable. Such measurements could be performed with a dedicated detector at a neutron spallation source [25].

In the hybrid model, the total reaction cross section consists then of two parts

$$\sigma_\nu^{tot}(E_\nu) \;=\; \sigma_\nu^{sm}(E_\nu) \,+ \sigma_\nu^{rpa}(E_\nu), \tag{1}$$

where the shell model part, σ_ν^{sm}, describes the Gamow-Teller contributions to the cross section, while the contributions from all other multipoles are comprised in the RPA part, σ_ν^{rpa}. The total cross section (denoted as 'cross section' in the following) is a function of the initial neutrino energy. We also calculate cross sections as a function of initial and final neutrino energies (called 'differential cross sections' below), obtained by gating $\sigma_\nu^{tot}(E_\nu)$ on a range of outgoing neutrino energies $[E'_\nu - \Delta E_\nu, E'_\nu)$ for a given energy of the incoming neutrino, E_ν. In principle, supernova simulations require the inelastic neutrino cross sections also as a function of angle of the final neutrino. The hybrid model allows the calculation of such differential cross sections. However, we have omitted this degree of freedom here, since supernova simulations can already judge the importance of inelastic neutrino-nucleus scattering on the basis of the differential cross sections and assuming an isotropic angular distribution.

As discussed above, finite-temperature effects will modify the Gamow-Teller contribution to the cross section. However, an explicit calculation of the cross section by shell model diagonalization at finite temperature ($T \gtrsim 1$ MeV) includes too many states to derive the GT strength distribution for each individual state and is hence unfeasible. We, therefore, use the same strategy as in [8]. We split the shell model cross section into parts describing i) neutrino down-scattering ($E'_\nu \leq E_\nu$) and ii) up-scattering ($E'_\nu \geq E_\nu$); here E'_ν, E_ν are neutrino energies in the final and initial states, respectively. For the down-scattering part we apply Brink's hypothesis which states that for a given excited nuclear level i the GT distribution built on this state, $S_i(E)$, is the same as for the ground state, $S_0(E)$, but shifted by the excitation energy E_i: $S_i(E) = S_0(E - E_i)$. Brink's hypothesis was proved valid if many states contribute to the thermal nuclear ensemble [26]. Upon applying Brink's hypothesis, the down-scattering part becomes independent of temperature and can be solely derived from the ground state GT distribution. With this approximation,

the Gamow-Teller (shell model) contribution to the cross section becomes:

$$\sigma_\nu^{sm}(E_\nu) = \frac{G_F^2}{\pi}\left[\sum_f E'^2_{\nu,0f}\, B_{0f}(GT_0) \;+\; \sum_{if} E'^2_{\nu,if}\, B_{if}(GT_0)\,\frac{G_i}{G}\right], \tag{2}$$

where G_F is the Fermi constant, and $E'_{\nu,if}$ is the energy of the scattered neutrino, $E'_{\nu,if} = E_\nu + (E_i - E_f)$, with E_i, E_f denoting the initial and final nuclear energies. The GT reduced transition probability between the initial and final nuclear states are given by

$$B_{if}(GT_0) \;=\; \left(\frac{g_A}{g_V}\right)^2_{eff} GT_0 \;=\; \left(\frac{g_A}{g_V}\right)^2_{eff} \frac{|\langle i||\sum_k \vec{\boldsymbol{\sigma}}^k \boldsymbol{t}_0^k||f\rangle|^2}{(2J_i+1)} \tag{3}$$

where the matrix element is reduced with respect to the spin operator $\vec{\boldsymbol{\sigma}}$ only and the sum runs over all nucleons; $\boldsymbol{t}_0$ is the zero-component of the isospin operator in a spherical representation. As required in $0\hbar\omega$ shell model calculations, the GT matrix elements have to be scaled by a constant quenching factor. We use [27]

$$\left(\frac{g_A}{g_V}\right)_{eff} \;=\; 0.74\,\left(\frac{g_A}{g_V}\right)_{bare}$$

with $(g_A/g_V)_{bare} = -1.2599(25)$ [28].

The first term in eq. (2) arises from Brink's hypothesis. By construction, this term does not allow neutrino up-scattering. These contributions to the cross section are comprised in the second term, where the sum runs over both initial (i) and final states (f). The former have a thermal weight of $G_i = (2J_i+1)\exp(-E_i/T)$, where J_i is the angular momentum, E_i is the energy of the initial state, and T is the temperature in MeV; $G = \sum_i G_i$ is the nuclear partition function. The up-scattering contributions are the more important i) the lower the nuclear excitation energy (the Boltzmann weight in the thermal ensemble regulates the population of the states), ii) the larger the GT transition strength B_{if}, and iii) the larger the final neutrino energy, $E'_{\nu,if}$. Guided by these general considerations we approximate the second term in eq. (2) by explicitly considering GT transitions between nuclear states with $E_i > E_f$, where the sum over the final nuclear states is restricted to the lowest (four to nine) nuclear levels. The respective GT matrix elements are determined by an 'inversion' of the shell model GT distributions of these low-lying states, employing a Lanczos diagonalization technique with 35-60 iterations per final angular momentum and isospin. Although the Lanczos states at moderate energies $E \gtrsim 4$ MeV represent the energy distribution of the strength, rather than converged nuclear states, the chosen ensemble of final nuclear states appears sufficient to approximate the nuclear partition function at the temperatures studied here. The lowest shell model energies were replaced by experimental data [29], whenever available.

The contributions of higher multipoles with rank $\lambda > 0$ to the cross section, σ_ν^{rpa} in eq. (1), were calculated using a generalized version of the RPA, which allows for partial occupancies of the single-particle orbits in the parent ground state. We have

taken the proton and neutron occupation numbers from the Independent Particle Model, which has been shown to yield quite similar cross sections for multipoles with $\lambda > 0$ as an approach where the shell model occupation numbers were used [21]. The RPA energies were derived from an appropriate Woods-Saxon potential, adjusted to reproduce the experimental values of the proton and neutron separation energies. As the residual interaction in the RPA calculation we adopted a zero-range Migdal force. The RPA formalism and its application to neutrino-nucleus reactions is described in detail in Refs. [4,18,30].

3 Results

Our study covers neutral-current neutrino reactions on the nuclei $^{50-60}$Mn, $^{52-61}$Fe, $^{54-63}$Co, and $^{56-64}$Ni, which are quite abundant during the supernova evolution. Furthermore, large-scale shell model calculations for the Gamow-Teller strength distributions can be performed for these nuclei. We present our results in three subsections. The Gamow-Teller distributions for the ground states, which determine the temperature-independent shell model contribution to the cross-section (first term in eq. (2)) are discussed in subsection 3.1. As we pointed out above, the thermal population of nuclear excited states influences the cross sections. We give examples of this dependence for three typical supernova temperatures in subsection 3.2. The differential cross sections are discussed in subsection 3.3, where we also compare the contributions of the down-scattering and up-scattering neutrino processes.

The cross-sections were calculated for larger ranges of temperature and neutrino energies than presented here. The full set of data is available from the corresponding author upon request.

3.1 GT_0 ground state transition strength

The relevant nuclear structure information resides in the matrix elements $B_{if}(GT_0)$, that define the strength for the Gamow-Teller operator $\vec{\boldsymbol{\sigma}}\boldsymbol{t}_0$ between initial and final states, see eq. (2). These matrix elements were taken from large-scale shell model calculations in the pf-shell using the computer code Antoine [31] and taking a slightly modified version of the KB3 residual interaction [14]. Some of these calculations were reported in Ref. [14] and were already used in several other neutrino-nucleus reaction studies for both charged- and neutral-current calculations: Toivanen *et al* [21] presented the total cross sections on $^{52-60}$Fe for the temperature $T = 0$ assuming several distributions of supernova neutrinos and antineutrinos. Sampaio *et al* [32] discussed neutrino and antineutrino absorption cross sections on ^{59,61}Fe, ^{60,62}Co, and ^{60,62}Ni. The total cross-sections and normalized neutrino spectra for neutral-current neutrino reactions on ^{56,59}Fe and ^{56,59}Co were presented in Ref. [8].

In Figs. 1-4 we present the GT_0 strength distributions for the various isotope chains;

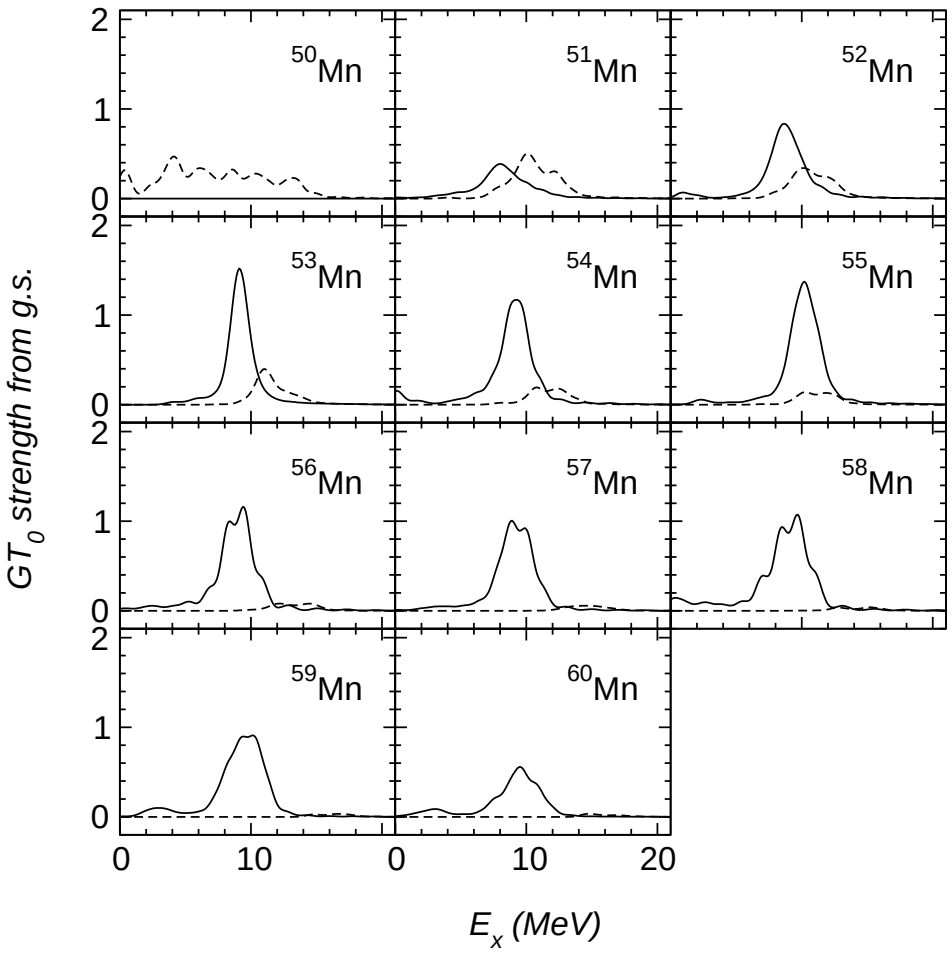

Fig. 1. Gaussian-smoothed neutral Gamow-Teller (GT_0) distributions from the ground states in Mn isotopes. Solid lines indicate $\Delta I = 0$ strength, and dashed lines - $\Delta I = 1$. E_x is the nuclear excitation energy, $E_x = E_i - E_{gs}$.

these strength distributions determine the temperature-independent shell model contribution to the cross section (the first term in eq. (2)). The neutral Gamow-Teller operator, $\vec{\boldsymbol{\sigma}}\boldsymbol{t}_0$, connects state (J_i, I_i) with the states $J_f - J_i = 0, \pm 1$ (but not $J_i = J_f = 0$) and $I_f - I_i = 0(\Delta I = 0), \pm 1(\Delta I = 1)$. Thus $\Delta I = 0$ transitions involve a change in the angular momentum, $J_f - J_i = 0, \pm 1$, but not in isospin. The $\Delta I = 1$ transition may have a lower $(I_i - 1)$ or higher $(I_i + 1)$ isospin in addition to a change in the angular momentum. As the odd-odd $N = Z$ nuclei ^{50}Mn and ^{54}Co have ground state isospin $I = 1$, both $\Delta I = 1$ components can contribute to the GT distribution in these nuclei. For all other nuclei, $\Delta I = 1$ allows only $I_f = I_i + 1$ transitions from the ground state. Furthermore, there is no $\Delta I = 0$ transition strength from the ground states of all $N = Z$ nuclei, as the relevant isospin Clebsch-Gordon coefficients ($\langle 0010|00\rangle$ and $\langle 1010|10\rangle$) vanish. We have distinguished the two isospin components of the GT_0 strength distribution in

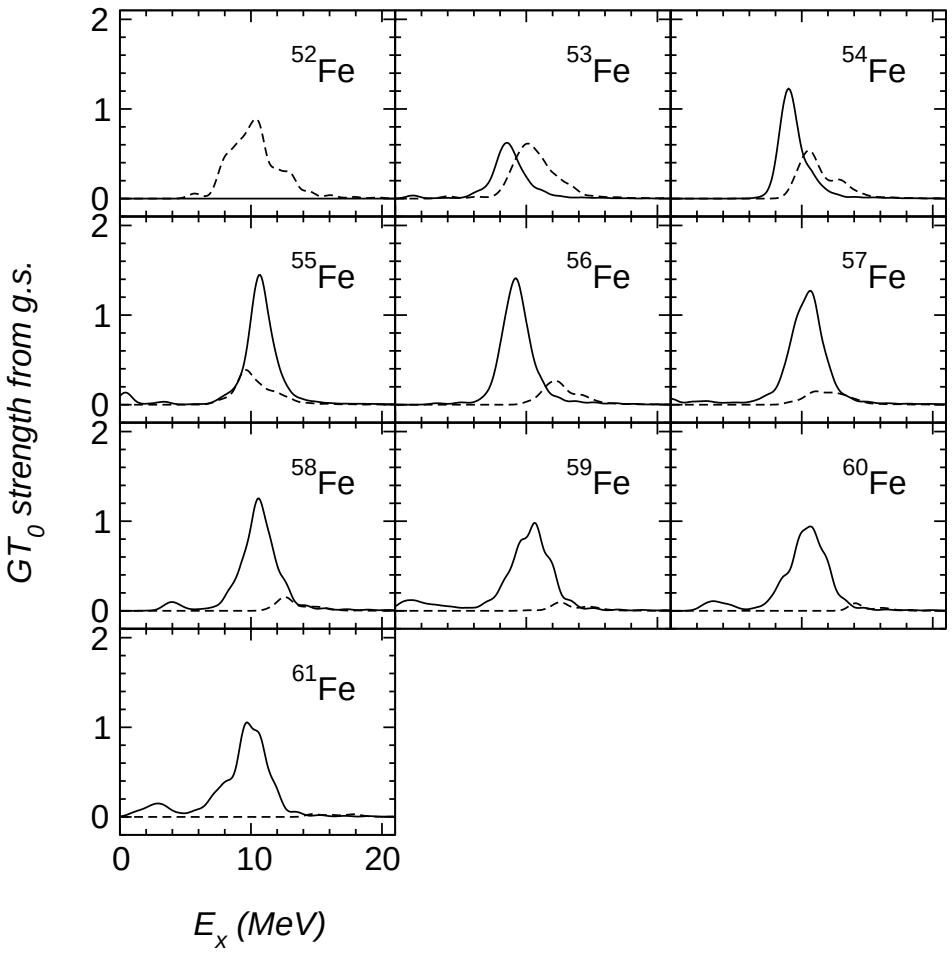

Fig. 2. Same as Fig. 1, but for Fe isotopes.

Figs. 1-4, where solid lines refer to the $\Delta I = 0$ part, and dashed lines show the transition strengths where the isospin changes by 1 unit.

We observe from Figs. 1-4 that the peak of the $\Delta I = 0$ ($I_i \rightarrow I_i$) GT_0 strength is at 8-12 MeV, while the strongest $\Delta I = 1$ ($I_i \rightarrow (I_i + 1)$) transitions lie a bit higher, in the energy range of 10-15 MeV. The position of the centroid does not indicate a pronounced sensitivity to the pairing structure of the ground state (see also [26,21]). The GT_0 strength for even-even nuclei is mainly concentrated in the resonance at around $\sim$ 10 MeV, while some low-lying strength in the Fe and Ni isotopes develops once nucleons start to occupy higher orbitals. Odd-A and odd-odd nuclei usually show some low-lying strength. The GT_0 strength distributions for the two odd-odd $N = Z$ nuclei ^{50}Mn and ^{54}Co are significantly more fragmented than the distributions for all other nuclei which is caused by the unusual isospin structure of these two nuclei.

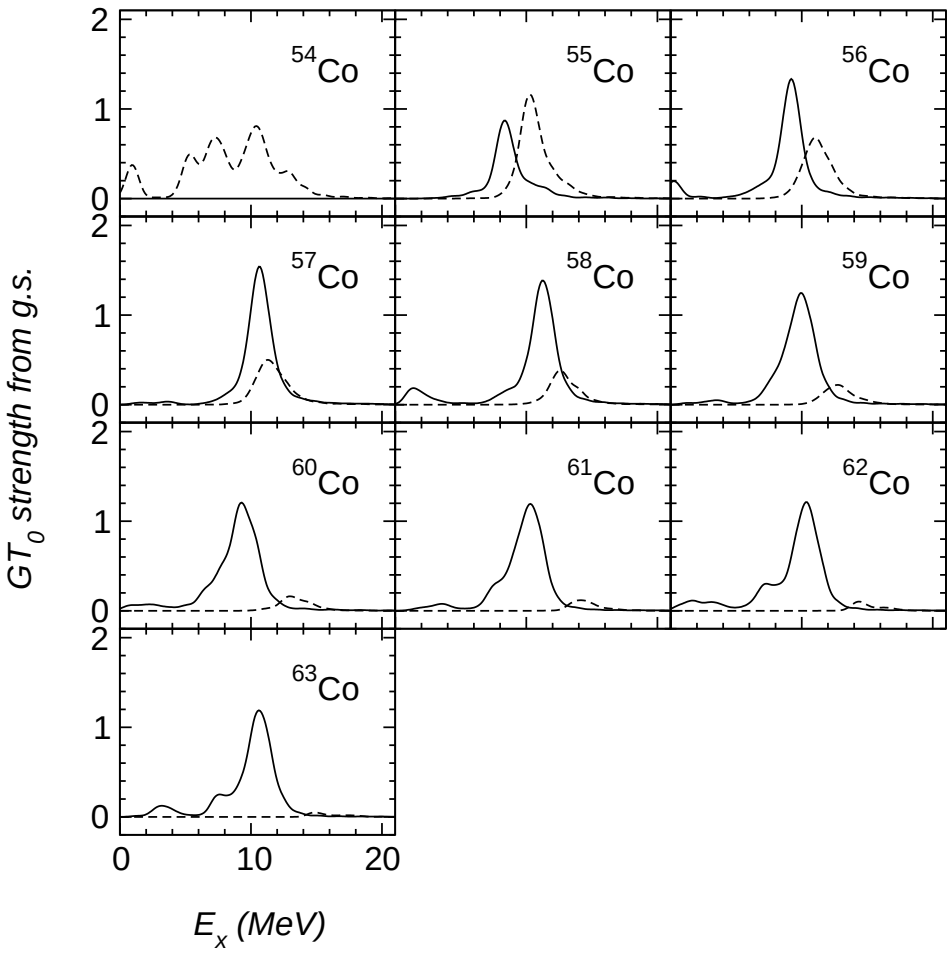

Fig. 3. Same as Fig. 1, but for Co isotopes.

Differences of our GT_0 strength distributions to those presented in [8,21] are related to different binning and smoothing. Furthermore, our figures do not show the 'elastic' (i.e. at $E_x = 0$) contribution to the strengths.

Our calculations of the down-scattering contribution to the cross-section (the first term in eq. (2)) is built on the Brink hypothesis. To test this assumption we plot in Figs. 5 and 6 the GT_0 strength distribution for a few low-lying states, adopting the nuclei ^{59}Mn and ^{60}Ni as examples. The figures support the validity of the Brink hypothesis for the centroid of the strength distribution, in agreement with the original formulation of the hypothesis for the collective states. We note, however, that the Brink hypothesis is not applicable for low-lying transitions of single-particle nature, as has already been discussed in Ref. [26].

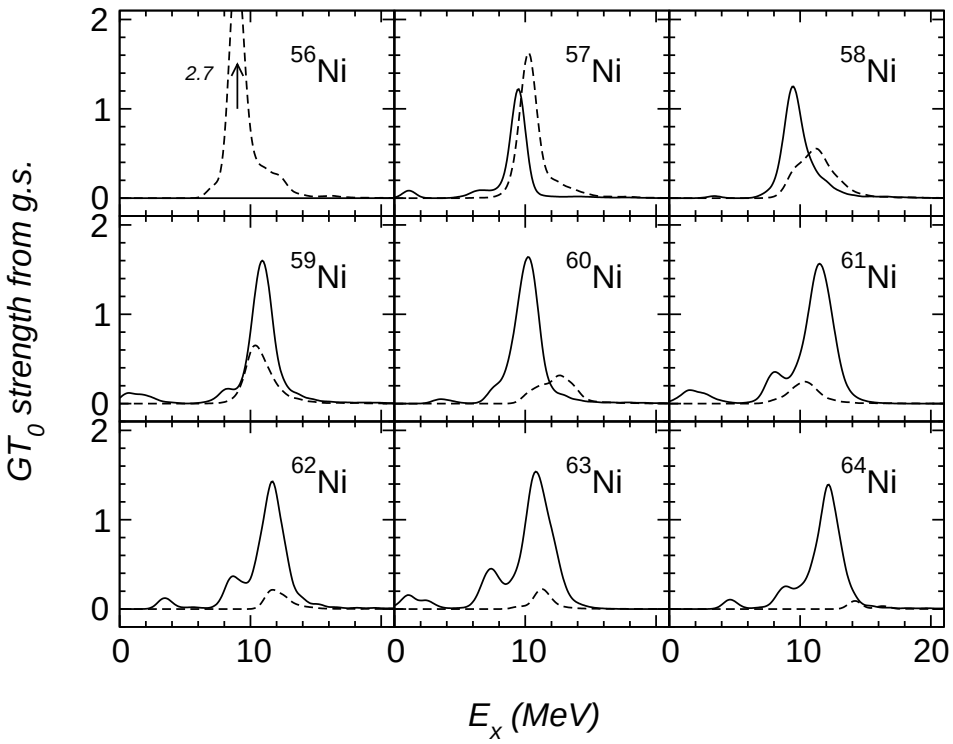

Fig. 4. Same as Fig. 1, but for Ni isotopes. The distribution peak in ^{56}Ni is at $E_x \sim 9$ MeV and reaches the value of 2.7.

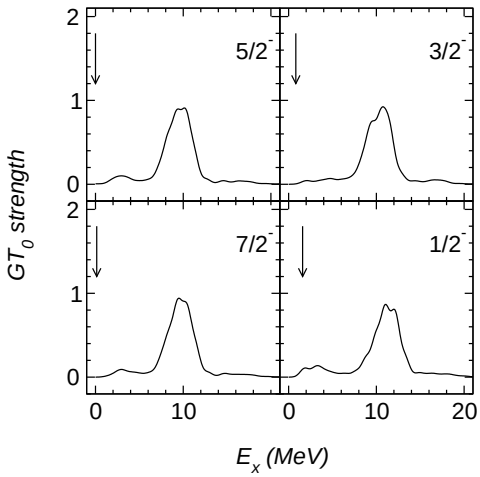

Fig. 5. Gamow-Teller distributions from the 4 lowest states in ^{59}Mn. An arrow indicates the calculated excitation energy of a state.

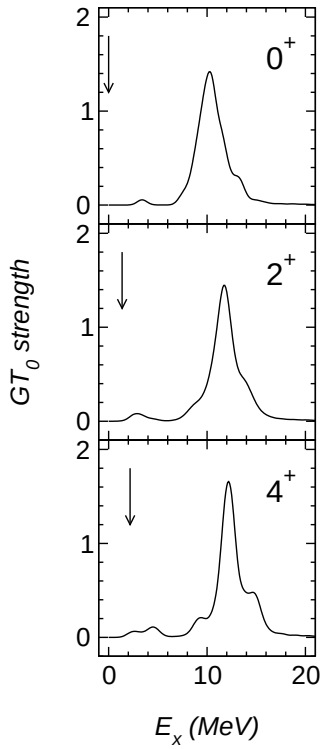

Fig. 6. Gamow-Teller distributions for 3 states in ^{60}Ni. See also caption of Fig. 5.

3.2 Thermal total cross-sections

As outlined in section 2, the contributions to the cross-sections arising from allowed transitions, $\lambda = 0$, and higher multipoles, $\lambda > 0$, are calculated within two different models: the shell model and RPA, respectively. Further, we assume that the contributions from the higher multipoles are temperature-independent. Thermal effects, which are included via Gamow-Teller deexcitations to the ground state and to low-lying excited states, are included in the shell model part of the cross section (second term in eq. (2)). Figs. 7-10 show the inelastic neutrino-nucleus cross sections for three different nuclear temperatures relevant for supernova physics: $T = 0.86$ MeV (10^{10} K), 1.29 MeV (1.5×10^{10} K), and 1.72 MeV (2×10^{10} K). The temperature $T = 0.86$ MeV corresponds to the condition in the core of a presupernova model for a $15M_\odot$ star ($\rho \sim 10^{10}$ g/cm^3 [33]). The two other temperatures relate approximately to neutrino trapping ($T = 1.29$ MeV) and thermalization ($T = 1.72$ MeV). For use in supernova simulations we have prepared cross section files for wider ranges of nuclear temperatures (from $T = 0.4$ to 2.0 MeV) and neutrino energies (from $E_\nu = 0$ to 100 MeV).

A previous study of neutral current neutrino-nucleus reaction cross-sections [8] suggested that finite-temperature effects are only relevant at low neutrino energies,

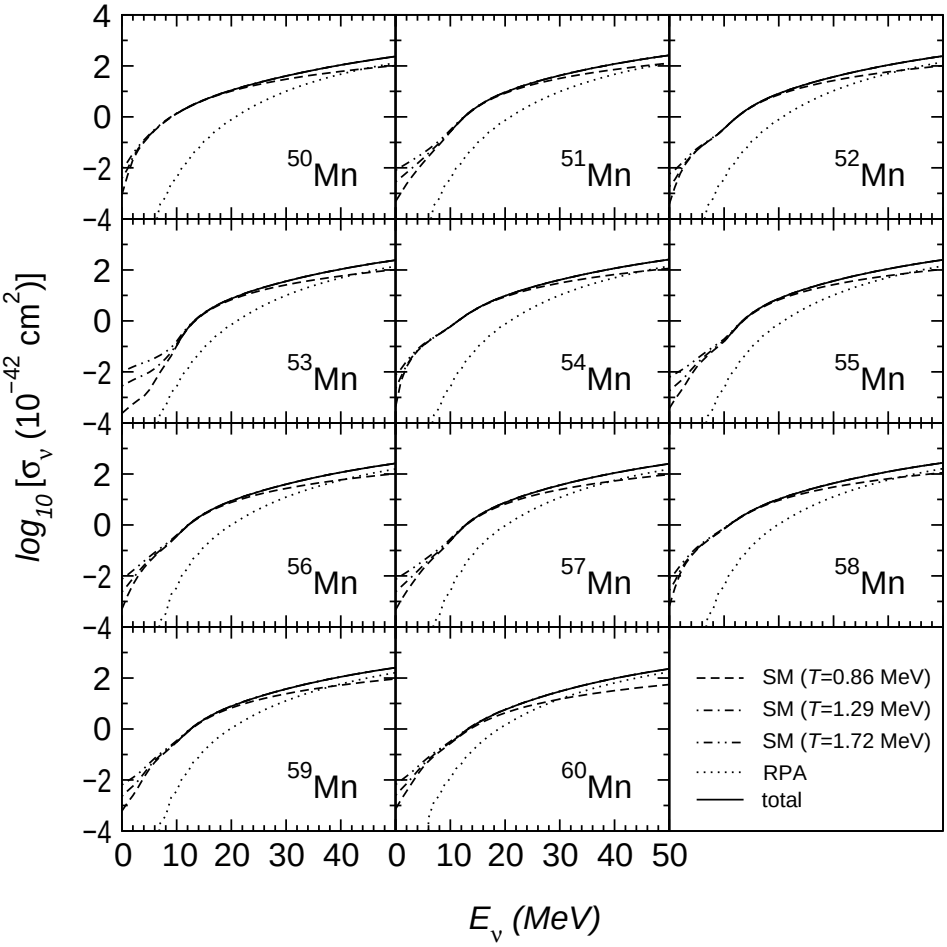

Fig. 7. Neutral current neutrino-nucleus inelastic cross-sections for Mn isotopes at different temperatures. Also shown is the RPA contribution to the cross section. At low neutrino energies the total cross section coincides with the shell model contributions.

$E_\nu \lesssim 10$ MeV. This is related to the energy of the GT_0 centroid which is located around 10 MeV. Once neutrinos have sufficienly large energies to excite the GT_0 centroid, the cross section is dominated by this transition. Furthermore, as for excited states the relative excitation energy of the centroid $(E_f - E_i)$ is about the same as for the ground state, the cross section becomes independent of temperature once transitions to the GT_0 centroid dominate the cross section. At high neutrino energies, other multipoles contribute to the cross section as well, where the excitation is again mainly due to the collective excitations. For these collective excitations, the Brink hypothesis applies again and the contributions of the forbidden multipoles to the cross section becomes temperature-independent.

At low neutrino energies, however, the cross section is temperature dependent and

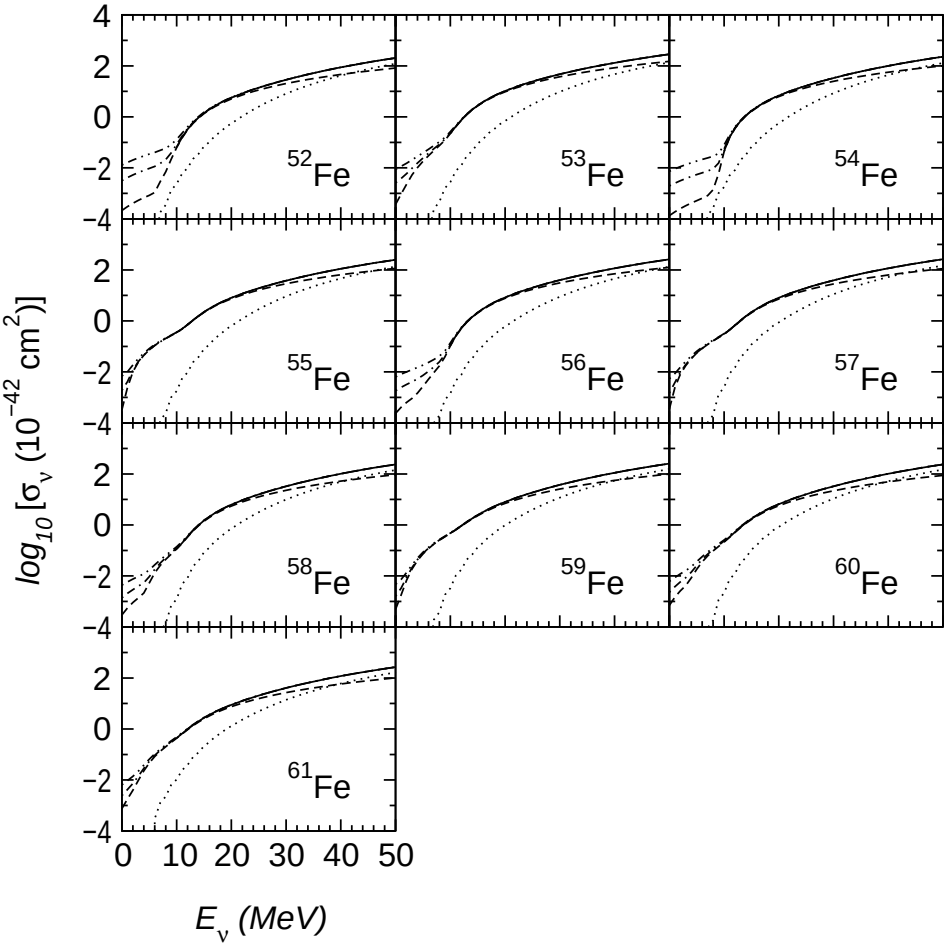

Fig. 8. Same as Fig. 7, but for Fe isotopes.

factors like the density of low-lying states and the GT_0 transition strength between such states become important. In general, odd-A and odd-odd nuclei have more low-lying states than even-even nuclei, where a gap between the ground state and the first excited state exists due to the isovector pairing. Furthermore, the ground states of even-even nuclei have angular momentum $J = 0$. GT_0 transitions can only connect these ground states to $J = 1$ states which usually exist at moderate excitation energies. This angular momentum mismatch creates a gap in the GT_0 strength distribution, which translates into an energy threshold for inelastic neutrino scattering at zero temperature. GT_0 transitions for excited states usually do not show such a gap, as due to the increased density of states in their vicinity the angular momentum mismatch is also absent. As a consequence, there is no neutrino threshold energy at finite supernova temperatures and low-energy inelastic neutrino cross sections on even-even nuclei are quite sensitive to temperature. As $E'_\nu < E_\nu$ in inelastic scattering on a ground state, a neutrino threshold energy also exists in odd-A and odd-odd nuclei. However, as these nuclei have a higher density of

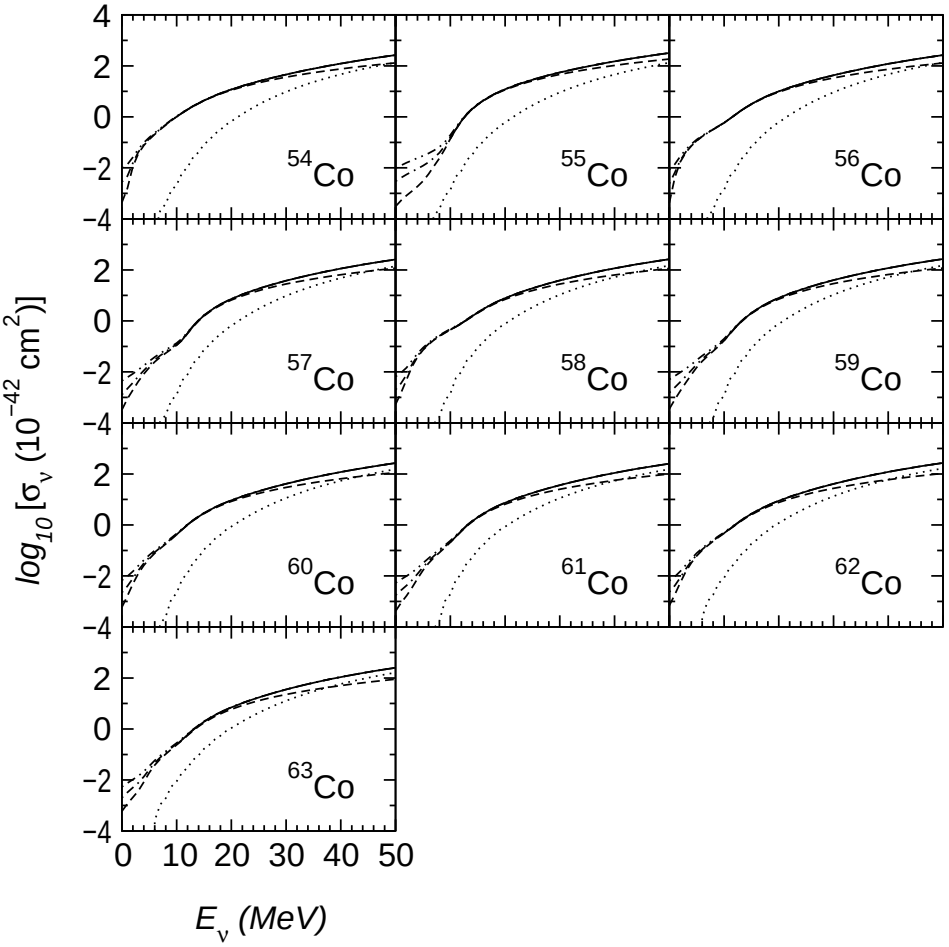

Fig. 9. Same as Fig. 7, but for Co isotopes.

low-lying states and an angular momentum mismatch is usually missing, the energy threshold for odd-A and odd-odd nuclei is much smaller than for even-even nuclei. As a consequence, generally one expects that temperature effects play a less important role for odd-A and odd-odd nuclei than for even-even nuclei [8]. However, due to nuclear structure effects there are exceptions to this general rule. The nuclei ^{53}Mn (see Fig. 7) and ^{55}Co (Fig. 9) are good examples of odd-even nuclei, where thermal effects are as important as in the even-even nucleus ^{56}Fe (Fig. 8). This is related to the fact that ^{53}Mn and ^{55}Co have a closed $f_{7/2}$ neutron shell in the non-interacting shell model picture, which reduces the density of low-lying states significantly.

We note that thermal effects can increase the low neutrino energy cross sections for even-even nuclei (and the closed neutron shell nuclei ^{53}Mn and ^{55}Co) by up to two orders of magnitude as the temperature raises from 0.86 MeV to 1.72 MeV. However, this effect is noticeably milder in nuclei like ^{60}Fe, where the GT_0 strength distribution for the ground state exhibits some low-lying strength. We discuss the

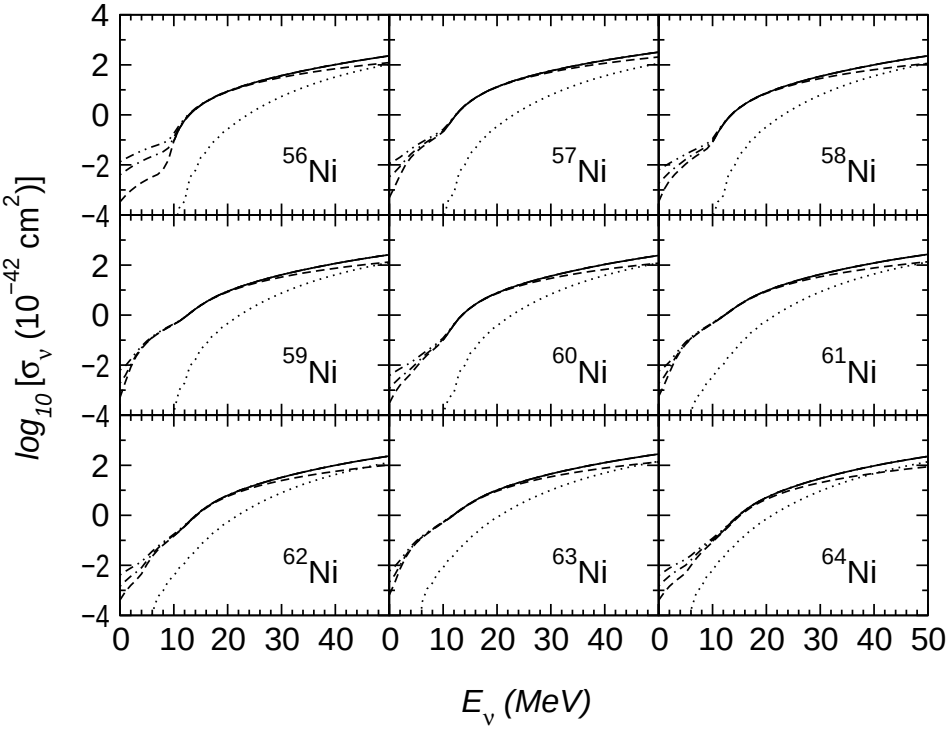

Fig. 10. Same as Fig. 7, but for Ni isotopes.

relative importance of thermal effects in a greater detail in the next subsection.

Sampaio *et al* studied inelastic neutrino scattering off ^{56,59}Fe and ^{56,59}Co [8]. In Fig. 11 we compare our results with those presented in Ref. [8]. There are three differences between our study and the previous one: we do not include elastic transitions, replaced our calculated low-excitation energies by experimental values whenever available [29], and calculated the value of the total partition function G more accurately. As [8] only considered Gamow-Teller contributions to the cross sections, we omit the contributions of higher multipoles to our cross sections in Fig. 11. The greatest difference is in the ^{59}Co cross-section, attributed to the omission of the strong elastic transition from the ground state. (This omission is also the reason for the difference between normalized neutrino spectra in ^{59}Co as shown in Figs. 3 and 4 of Ref. [8] and our Fig. 14 below.)

At low neutrino energies the cross-sections are almost completely given by the allowed (GT_0) contribution. However, contributions arising from forbidden multipoles become increasingly important at larger neutrino energies. We find that, for $E_\nu = 20$ MeV neutrinos, up to 18% of the cross sections is due to the forbidden transitions (in ^{60}Mn this is 24%). For $E_\nu \sim$ 30-50 MeV allowed and forbidden transitions contribute about equally to the cross section, while at $E_\nu = 100$ MeV the cross sections are dominated by forbidden multipoles, with the GT_0 contributing about 15-20%.

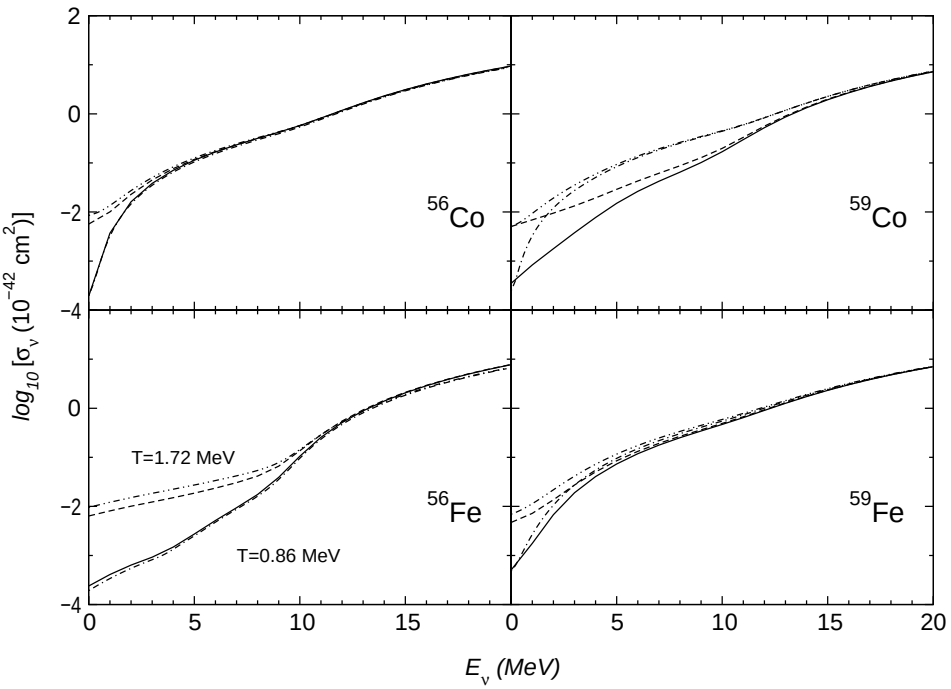

Fig. 11. Comparison of the calculated shell model cross sections with those presented in Fig. 2 of Ref. [8]. The solid and dashed lines show the current calculations at temperatures $T = 0.86$ and 1.72 MeV, respectively; the dash-dotted and dash-double-dotted lines show results from Ref. [8] for the same temperatures.

3.3 Differential cross sections

Among all reactions induced by neutrinos during the supernova collapse the rate for elastic scattering of (electron) neutrinos on nuclei is largest. As this process involves momentum transfer (but no energy transfer), it randomizes the neutrino escape path from the collapsing core and ultimately leads to the neutrino trapping and the formation of the homologuous core (see e.g. [12]). Thermalization of neutrinos and supernova matter is made possible by neutrino processes involving energy exchange. As mentioned above, inelastic neutrino-electron scattering is until now considered as the dominating process, but inelastic neutrino-nucleus scattering, ignored so far, could be quite important as well [12]. We have calculated the relevant partial differential cross sections for the various Mn, Fe, Co, and Ni isotopes, covering initial neutrino energies in the interval between $E_\nu = 2$ and 60 MeV in 2 MeV steps and in the interval $E_\nu = 60$-100 MeV in 4 MeV steps. The cross sections are then gated into 1 MeV bins for the final neutrino energies for $E'_\nu < 50$ MeV, and 2 MeV bins for $E'_\nu = 50$-100 MeV. While a table with a complete data set for all 40 individual nuclei is available upon request from the corresponding author, we would like to discuss general results and a few examples for the partial cross sections in this subsection. For given neutrino energies we will present our results as spectra

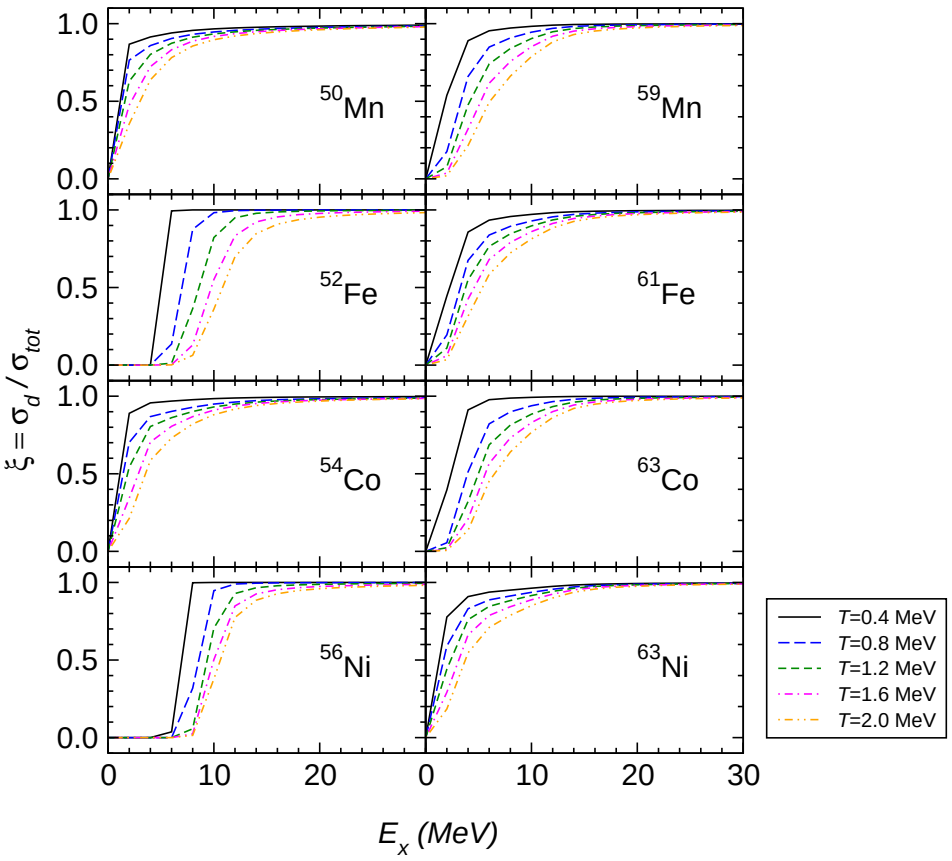

Fig. 12. (Color online) Temperature dependence of the fraction of down-scattered neutrinos for selected nuclei: ^{50,59}Mn, ^{52,61}Fe, ^{54,63}Co, and ^{56,63}Ni. The sharp transitions are due to a coarse energy grid.

for the neutrinos in the final state.

As discussed in the previous subsection, inelastic neutrino-nucleus cross sections for low-energy neutrinos are increased by thermal effects. At higher neutrino energies $E_\nu \gtrsim 10$ MeV, the main contribution to the cross-section comes from the Gamow-Teller excitation, which resides at excitation energies around 10 MeV. Under these circumstances neutrino down-scattering becomes the dominating process. Temperature effects (neutrino up-scattering) are no longer important at $E_\nu \gtrsim 15$ MeV. This general behavior can be visualized by introducing the ratio ξ of the down-scattering cross section, σ_d, and the total cross section, $\sigma_{\rm tot}$:

$$\xi = \frac{\sigma_d}{\sigma_{\rm tot}} = 1 - \frac{\sigma_u}{\sigma_{\rm tot}}, \tag{4}$$

where the up-scattering cross section $\sigma_u(E_\nu)$ is given by the second term in eq. (2).

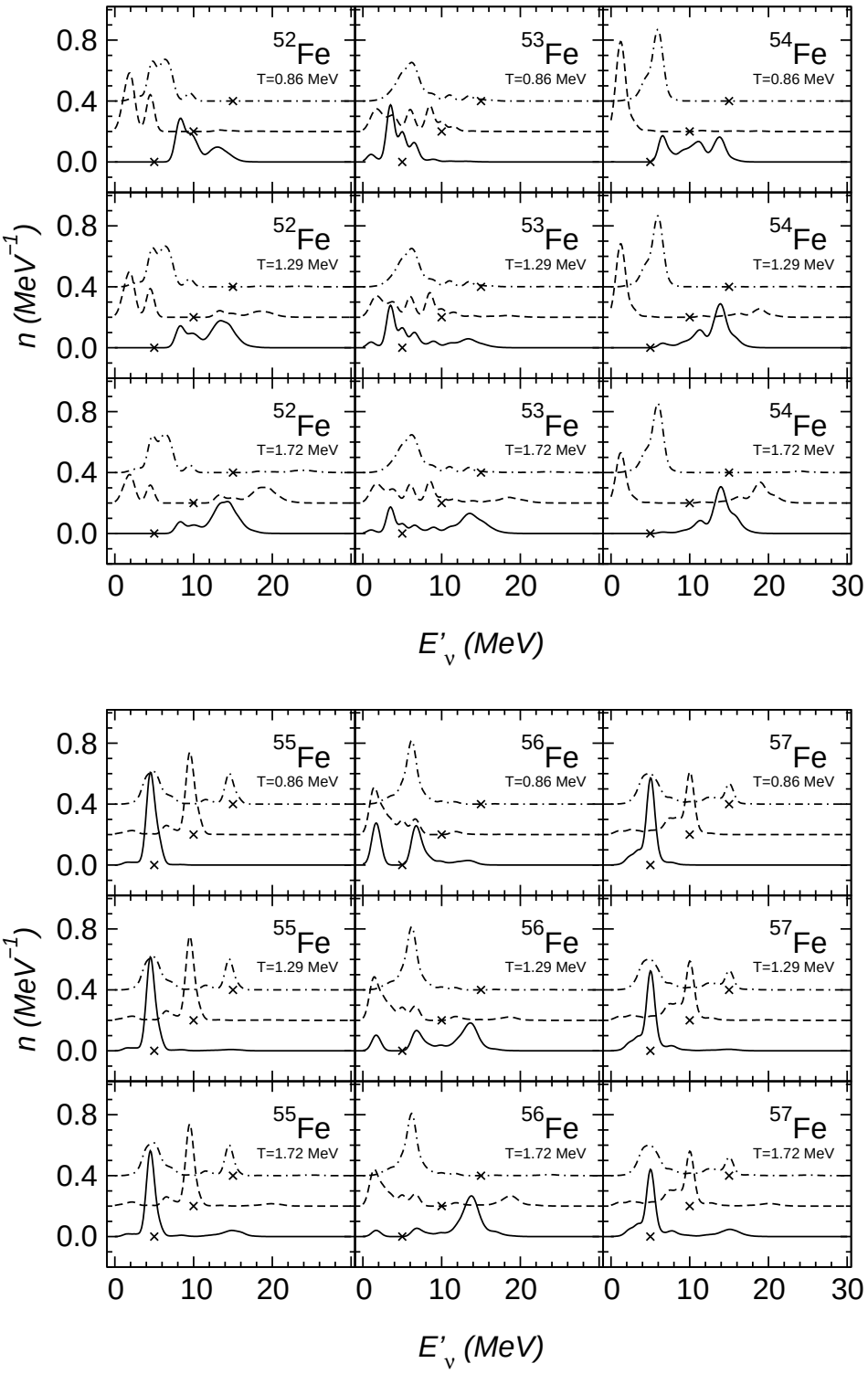

Fig. 13. Normalized spectra for final neutrino energies in inelastic neutrino scattering on $^{52-57}$Fe for three temperatures ($T = 0.86$, 1.29, and 1.72 MeV) and three initial neutrino energies: $E_\nu = 5$ MeV (solid line), 10 MeV (dashed line, all values shifted by 0.2), and 15 MeV (dash-dotted line, all values shifted by 0.4). Crosses correspond to the energy of the incoming neutrino.

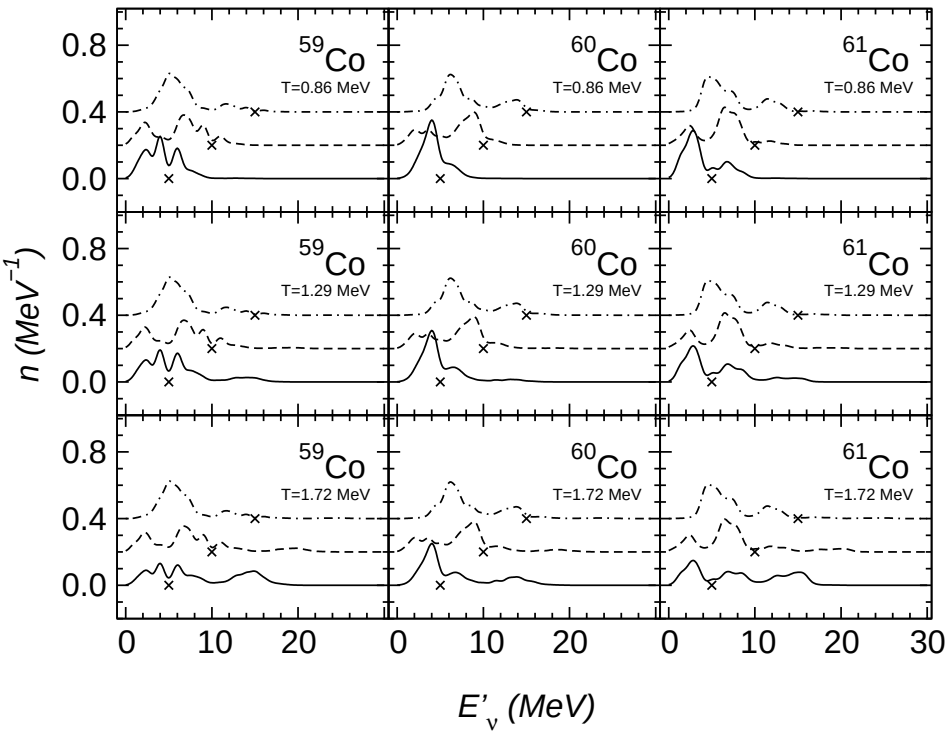

Fig. 14. Same as Fig. 13 but for ^{59,60,61}Co

In Fig. 12 we plot the ratio ξ as a function of the initial neutrino energy for selected temperatures and nuclei. As expected, the ratio $\xi \sim 1$ is usually obtained for $E_\nu = 15$ MeV and temperature effects become unimportant. (For some nuclei, like ^{52}Fe and ^{56}Ni, temperature effects persist to neutrino energies slightly larger than 15 MeV.) At low neutrino energies we observe differences between the individual nuclei, caused by the nuclear structure effects discussed above.

In the previous subsection we outlined that even-even nuclei (and certain others) have sizable energy thresholds for inelastic neutrino scattering off the ground state. For these nuclei thermal effects are more important and, obviously, they are more likely to up-scatter low-energy neutrinos than those where the threshold is virtually absent. This can be seen in Fig. 12, and we also demonstrate this behavior for the nuclei $^{52-57}$Fe and $^{59-61}$Co in Figs. 13 and 14. For each nucleus we present the normalized-to-unity neutrino spectra at three different temperatures ($T = 0.86$, 1.29, and 1.72 MeV) and, for each temperature, for three different initial neutrino energies are shown: $E_\nu = 5$, 10, and 15 MeV.

As the spectra in Figs. 13 and 14 are normalized, the increase in absolute magnitude with temperature is not reflected, but can be read off Figs. 7-10. We remind here that in our formulation of the total cross section, only the up-scattering processes ($E'_\nu > E_\nu$) are temperature-dependent. The absolute value of the neutrino up-scattering

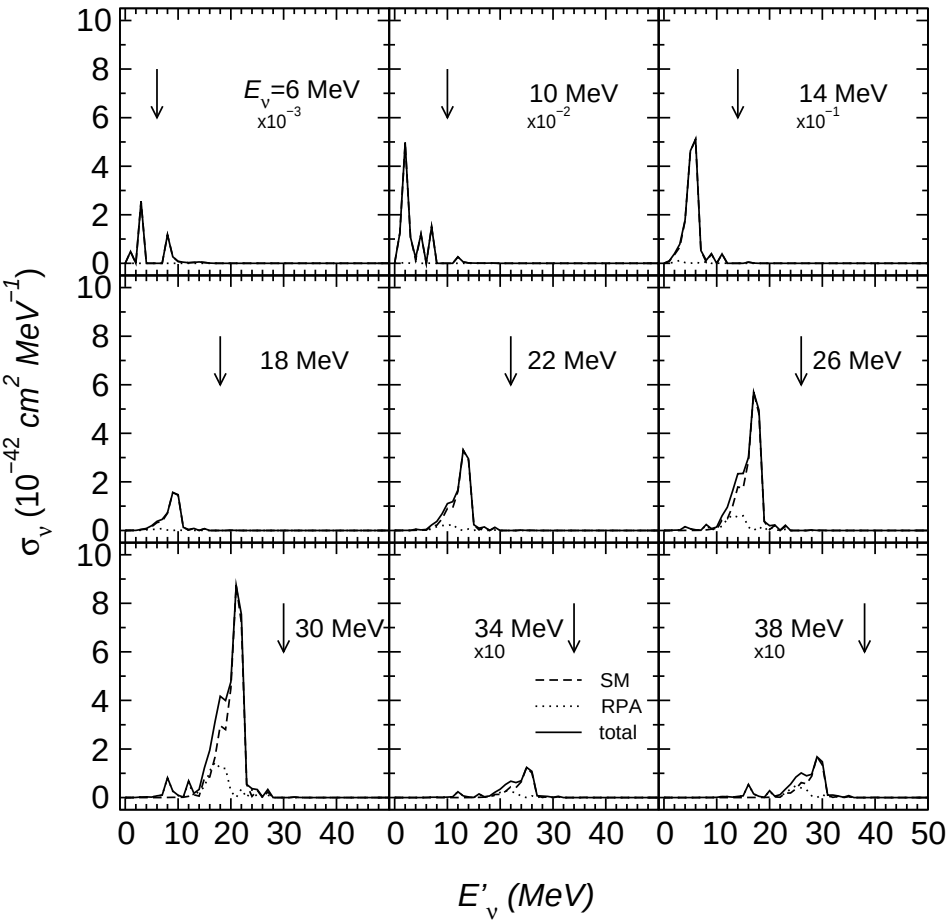

Fig. 15. Differential cross-sections for inelastic neutrino scattering on ^{56}Fe for nine different initial neutrino energies and $T = 0.8$ MeV. Each plot contains three lines: the dashed line shows the shell model, the dotted line - the RPA contributions, and the solid line shows the sum. For some E'_ν values, the entire cross section comes either from the shell model or RPA contributions alone. In all plots the energy of the incoming neutrino is indicated by an arrow. In some plots the cross sections have been scaled by the given factors (see text). The bin size is 1 MeV.

cross section increases with temperature since a larger fraction of nuclear excited states with increasing phase space can be populated. Consequently, the relative contribution of up-scattered neutrinos in the spectra increases with temperature and, for a given E_ν, the spectra of up-scattered neutrinos are getting wider as temperature increases.

The missing low-energy strength in the ground state GT_0 distributions for the even-even isotopes ^{52,54}Fe (Fig. 2) implies that these nuclei have only a very few states which can be excited by a $E_\nu = 5$ MeV neutrino. Therefore the neutrino distributions for these nuclei (Fig. 13) are dominated by up-scattered neutrinos even for

temperatures as low as $T = 0.86$ MeV. The up-scattering process dominates also in ^{56}Fe at $T = 1.29$ and 1.72 MeV, but it is about equally significant as down-scattering at $T = 0.86$ MeV. As expected from Fig. 12, a fraction of the $E_\nu = 10$ MeV neutrinos is up-scattered by even-even iron isotopes. For $E_\nu = 15$ MeV neutrinos, temperature effects are unimportant and nearly all neutrinos are down-scattered. As temperature effects are in general less important for odd-A nuclei, inelastic neutrino scattering on the odd isotopes ^{53,55,57}Fe up-scatter a much smaller fraction of neutrinos, even at $E_\nu = 5$ MeV, than scattering on even iron isotopes. Similarly, up-scattering is also relatively unimportant for odd-odd nuclei. This is demonstrated in Fig. 14, where we show the normalized neutrino spectra for the odd-Z isotopes $^{59-61}$Co. Although present for $E_\nu = 5$ MeV neutrinos, neutrino up-scattering is significantly less pronounced than for the even-even iron isotopes. When comparing the current neutrino spectrum for ^{59}Co with Fig. 3 in Ref. [8], one can observe that there is no big $E'_\nu \approx E_\nu$ contribution, which is related to the omission of the elastic contribution to the cross section here.

In Fig. 15 we show the (unnormalized) partial cross sections for inelastic neutrino scattering off ^{56}Fe, choosing $T = 0.8$ MeV as a representative supernova temperature. The partial cross sections cover the range of initial neutrino energies between $E_\nu = 6$ MeV and 38 MeV in 4 MeV steps. Note that for a clearer presentation, some of the cross sections are scaled (i.e. the actual values are obtained by multiplying the shown cross sections by the indicated factors, which, for example, is 10^{-3} for $E_\nu = 6$ MeV). At all shown initial neutrino energies the cross sections are dominated by the GT_0 contributions. As a consequence, the largest partial cross sections are found for $E'_\nu \sim (E_\nu - 10$ MeV) for $E_\nu > 10$ MeV, corresponding to the centroid of the GT_0 distribution. For higher neutrino energies we observe the appearance of structures in the partial cross sections at final neutrino energies smaller than corresponding to the GT_0 centroid. These peaks are related to excitations of the giant resonances in forbidden multipole transitions, which, as expected, become more prominent with increasing initial neutrino energies. To make this relation more visible, the figure shows the individual contributions of the allowed and forbidden multipole transitions to the partial cross sections.

4 Summary and conclusions

We performed studies of neutral-current neutrino-nucleus reactions for four isotope chains: Mn, Fe, Co, and Ni. These studies are relevant for supernova simulations and hence have to take the finite temperature of the supernova environment into account. In our approach, we determine the allowed contributions to the cross sections from large-scale diagonalization shell model evaluations of the Gamow-Teller GT_0 response. Contributions to the cross sections, arising from other multipoles, were calculated within the random-phase approximation. We have calculated the GT_0 distributions for many nuclei for the first time. Our results indicate a systematic trend in these distributions as they are usually dominated by a collective excitation whose centroid is located at excitation energies around 10 MeV in the nuclei stud-

ied here. Finite temperature effects on the cross sections are only relevant at rather small neutrino energies and were approximated in our approach by considering GT_0 transitions from thermally populated states to the ground state and excited states at low nuclear excitation energies.

We confirm the conclusions of Ref. [8] that finite temperature effects enhances the inelastic scattering cross-sections for low energy neutrinos. We also find that temperature effects become negligible once the energy of the initial neutrino is large enough to allow for transitions to the centroid of the GT_0. Furthermore, due to nuclear structure effects the temperature dependence is in general largest for even-even nuclei, and among the nuclei studied here, also for the two odd-A nuclei with closed $f_{7/2}$ neutron shells (^{53}Mn and ^{55}Co).

One goal of our study was to produce inelastic neutrino-nucleus cross sections suitable for use in supernova simulations. However, in the unshocked regions of supernova where this process is relevant, many nuclei are present in the matter composition with sizable abundance. Supernova simulations which contain detailed neutrino transport, however, represent this matter composition by protons, neutrons, α particles and 'average nuclei' which simulate all heavier nuclei, see e.g. [34]. For use in supernova simulations, the neutrino cross sections for the individual nuclei have to be averaged over the supernova matter composition, as it is, for example, done for stellar electron capture [35,3,9,10]. To simplify this procedure it has been proposed in Ref. [8] to determine the neutrino-nucleus cross sections from an 'average nucleus' which is chosen to approximate the matter composition. Such a prescription is justified by our calculations for larger neutrino energies, say at $E_\nu > 15$ MeV, where the cross sections for the various nuclei are rather similar. However, the prescription appears to be less justified at low neutrino energies where the cross sections for different nuclei show strong variations. For these neutrino energies it is preferable to calculate the total neutrino-nucleus cross section as a compositionally weighted average over the individual cross sections. This procedure is facilitated as the supernova matter composition is given by Nuclear Statistical Equilibrium under most conditions where the cross sections are needed.

Inclusion of these rates in a supernova simulation is beyond the scope of this paper. However, to get an idea of the importance of this process we estimated the heating rate in the post-bounce region using results from a previous simulation [10]. Following Bruenn and Haxton [12], we approximated the reaction cross sections on all nuclei in the iron-shell by one nucleus. To check the variations in the produced rates we took four different cases: ^{55}Co, ^{56}Co, ^{55}Fe, and ^{56}Fe. The obtained heating rates were different by 40-50%, supporting the idea that the neutrino-nucleus heating rate in supernova is moderately sensitive to the detailed composition of the region.

The astrophysical implications of these improved neutral-current neutrino-nucleus reaction rates are currently under investigation. Prior investigations by Bruenn and Haxton [12] found that the energy transfer due to neutrino-nucleus scattering was comparable to (but smaller than) that from neutrino-electron scattering during the infall phase. At later times in the simulation, Bruenn and Haxton found that while neutrino-nucleus scattering dominated in the cooler iron-rich regions, $\bar{\nu}_e$ capture on

protons and neutrino scattering on ^{4}He were more important closer to the shock. Given the similarity of our cross sections to those used by Bruenn and Haxton for the neutrino energy range of relevance for post-shock heating ($E_\nu \gtrsim 15$ MeV), we expect their conclusions to stand. However, in addition to the microscopic rates for the interactions themselves, these conclusions also depend strongly on the composition which depends on the hydrodynamic state and neutronization, since the matter in question is in Nuclear Statistical Equilibrium. Therefore these conclusions must be revisited in light of recent improvements in supernova models. Of particular interest in this regard is the impact of revisions in the treatment of nuclear electron capture [9,26] which have recently been shown to alter the thermodynamics and neutronization throughout the collapsing stellar core [10,33]. Improved cross-sections for ^{4}He (see, however, [36]), as well as intermediate mass nuclei, would be desirable, since these nuclei experience the intense neutrino flux in the supernova as well.

Acknowledgements

We thank M. Liebendörfer, A. Mezzacappa, S.W. Bruenn, and O.E.B. Messer for useful discussions of supernova simulation results. A.J. and W.R.H. are partially supported by the Department of Energy through the Scientific Discovery through Advanced Computing (SciDAC) program. W.R.H. is also supported in part by NSF under contract PHY-0244783. K.L. and J.M.S. are partially supported by the Danish Research Council. G.M.P. is supported by the Spanish MCyT and by the European Union ERDF under contracts AYA2002-04094-C03-02 and AYA2003-06128. J.M.S. acknowledges the financial support of the Portugese Foundation for Science and Technology. Oak Ridge National Laboratory is managed by UT-Battelle, LLC, for the U.S. Department of Energy under Contract No. DE-AC05-00OR22725 with UT-Battelle, LLC.

References

[1] H.A. Bethe, *Rev. Mod. Phys.* **62** (1990) 801.

[2] W.R. Hix, A. Mezzacappa, O.E.B. Messer, and S.W. Bruenn, *J. Phys.* **G 29** (2003) 2523.

[3] K. Langanke, and G.Martínez-Pinedo, *Rev. Mod. Phys.* **75** (2003) 819.

[4] E. Kolbe, K. Langanke, G. Martínez-Pinedo and P. Vogel, *J. Phys.* **G 29** (2003) 2569.

[5] A. Mezzacappa, M. Liebendörfer, O.E.B. Messer, W.R. Hix, F.-K. Thielemann, and S.W. Bruenn, *Phys. Rev. Lett.* **86** (2001) 1935.

[6] M. Rampp and H.-Th. Janka, *Astrophys. J.* **539** (2000) L33.

[7] R. Buras, M. Rampp, H.-Th. Janka, and K. Kifonidis, *Phys. Rev. Lett.* **90** (2003) 241101.

[8] J.M. Sampaio, K. Langanke, G. Martínez-Pinedo, and D.J. Dean, *Phys. Lett.* **B 529** (2002) 19.

[9] K. Langanke, G. Martínez-Pinedo, J.M. Sampaio, D.J. Dean, W.R. Hix, O.E.B. Messer, A. Mezzacappa, M. Liebendörfer, H.-Th. Janka, and M. Rampp, *Phys. Rev. Lett.* **90** (2003) 241102.

[10] W.R. Hix, O.E.B. Messer, A. Mezzacappa, M. Liebendörfer, J. Sampaio, K. Langanke, D.J. Dean, and G. Martínez-Pinedo, *Phys. Rev. Lett.* **91** (2003) 201102.

[11] S.W. Bruenn, *Astrophys. J. Suppl.* **58** (1985) 771.

[12] S.W. Bruenn and W.C. Haxton, *Astrophys. J.* **376** (1991) 678.

[13] W.C. Haxton, *Phys. Rev. Lett.* **60** (1988) 1999.

[14] E. Caurier, K. Langanke, G. Martínez-Pinedo, and F. Nowacki, *Nucl. Phys.* **A 653** (1999) 439.

[15] D. Frekers, *Nucl. Phys.* **A 731** (2004) 76.

[16] M. Hagemann *et al*, *Phys. Lett.* **B 579** (2004) 251.

[17] C. Bäumer *et al*, *Phys. Rev.* **C 68** (2003) 031303R.

[18] E. Kolbe, S. Krewald, K. Langanke, and F.-K. Thielemann, *Nucl. Phys.* **A 540** (1992) 599.

[19] E. Caurier, G. Martínez-Pinedo, F. Nowacki, A. Poves and A.P. Zuker, *nucl-th/0402046*.

[20] E. Kolbe, K. Langanke, and G. Martínez-Pinedo, *Phys. Rev.* **C 60** (1999) 052801.

[21] J. Toivanen, E. Kolbe, K. Langanke, G. Martínez-Pinedo, and P. Vogel, *Nucl. Phys.* **A 694** (2001) 395.

[22] B. Zeitnitz and KARMEN Collaboration, *Prog. Part. Nucl. Phys.* **32** (1994) 351.

[23] K. Langanke, G. Martínez-Pinedo, P. von Neumann-Cosel, and A. Richter, *nucl-th/0402001*.

[24] Y. Fujita *et al*, *Phys. Lett.* **B 365** (1996) 29.

[25] F.T. Avignone III, L. Chatterjee, Y.V. Efremenko, and M.R. Strayer, *J. Phys.* **G 29** (2003) 2497.

[26] K. Langanke and G. Martínez-Pinedo, *Nucl. Phys.* **A 673** (2000) 481.

[27] G. Martínez-Pinedo, A. Poves, E. Caurier, and A.P. Zuker, *Phys. Rev.* **C 53** (1996) R2602.

[28] I.S. Towner and J.C. Hardy, in: W.C. Haxton, E.M. Henley (Eds.), Symmetries and Fundamental Interactions in Nuclei, World Scientific, Singapore, 1995, p. 183.

[29] Online version of Nuclear Data Sheets: *http://ie.lbl.gov/ensdf/welcome.htm*

[30] E. Kolbe, K. Langanke, and P. Vogel, *Nucl. Phys.* **A 652** (1999) 91.

[31] E. Caurier, computer code ANTOINE, IReS, Strasbourg, 1989.

[32] J.M. Sampaio, K. Langanke, and G. Martínez-Pinedo, *Phys. Lett.* **B 511** (2001) 11.

[33] A. Heger, K. Langanke, G. Martínez-Pinedo, and S.E. Woosley, *Phys. Rev. Lett.* **86** (2001) 1678.

[34] J.M. Lattimer and F.D. Swesty, *Nucl. Phys.* **A 535** (1991) 331.

[35] G.M. Fuller, W.A. Fowler, and M.J. Newman, *Astrophys. J.* **252** (1982) 715.

G.M. Fuller, W.A. Fowler, and M.J. Newman, *Astrophys. J. Suppl.* **48** (1982) 279.

[36] D. Gazit and N. Barnea, *nucl-th/0402077*.